

Effects of width increase in the ballistic quantum wire

Toshihiro Itoh, Nobuyuki Sano, and Akira Yoshii

NTT LSI Laboratories, 3-1 Morinosato-wakamiya, Atsugi-shi, Kanagawa-ken 243-01, Japan

(Received 3 February 1992)

We investigate the effects of a width increase on the electronic properties of ballistic quantum wires by evaluating the local density of states and the conductance. A local widening of the quantum wire introduces dip structures in addition to the well-known steplike structures of the conductance. The mode coupling between the bound state and the extended state is the origin of these structures. The quasi-bound and the complete backscattering state are clearly shown to arise as a result of mode couplings. We also point out that a smooth variation of the width of the quantum wires does not remove these quasibound states.

Conductance quantization in the quantum point contact was discovered in 1987.¹ Because of its fundamental interest and practical importance in device application, transport characteristics of quasi-one-dimensional wires with various structures have been extensively investigated.^{2,3} Past work has shown that the widening of the boundary of the quantum wire has an intrinsic effect on the electronic transport properties. Sols *et al.*⁴ found that the dip structure appears in the conductance when the wire has a stub. Kasai *et al.*⁵ examined a quantum wire with a similar structure and claimed that the dip structure occurs when the electron energy coincides with that of the bound state. Nakazato *et al.*⁶ showed that in the double-constriction geometry the virtual bound state couples with the lower mode and that this is the origin of the resonant or antiresonant peaks. As the method of Nakazato *et al.* is restricted to the case where no real bound state exists, it is still not clear when the quasi-bound state or bound state arises and how it affects the conductance. Chu *et al.*,⁷ Bagwell,⁸ and Tekman *et al.*⁹ examined the effect of impurities introduced into the wire. They showed that a similar dip structure arises when the potential is attractive. But their explanations of the dip structures are rather qualitative and the existence of quasibound states has not yet been clearly shown. Moreover, the relation between the introduced potential and the width increase is still not clear.

In this paper we investigate the effects of a width increase on the electronic transport properties of ballistic quantum wires. The system that we treat is single width increase, which may be regarded as a simple model of width fluctuation. We show that the dip structures seen in such quantum wires are the result of mode couplings and clarify the properties of the arising quasibound state and of the complete backscattering state by evaluating the local density of states. We show that the mode couplings associated with width increase govern the lifetime of quasibound states and the width of the dip structure. Finally, we briefly discuss what happens when the width is changed adiabatically.

For numerical analyses we employed the (recursive) tight-binding Green-function method introduced by Sols

*et al.*⁴ This method is a slight modification of the conventional recursive Green-function method¹⁰ and is more efficient than the conventional one for analyzing the structures made up of simple parts in which the Green function can be analytically determined. The formulation is based on a one-electron picture and any many-body effects or inelastic scattering as well as impurity scattering are ignored.

Since electron transport is ballistic inside the wire, the Hamiltonian is given by the kinetic-energy term, $p^2/2m$, in the wire. In a two-dimensional tight-binding lattice, the Hamiltonian is expressed as

$$H = -V \sum_{\langle NN \rangle} (|i\rangle\langle j| + |j\rangle\langle i|) + E_0 \sum_i |i\rangle\langle i|, \quad (1)$$

where $|i\rangle$ is the state of the electron on the i th site [$i = \vec{r} = (r_x, r_y)$], and the sum in the first term is over all nearest-neighbor pairs of i and j . $V [= \hbar^2/(2m^*a^2)]$ is the transfer energy and $E_0 (= 4V)$ is a constant, where m^* is the effective electron mass and a is the lattice spacing of the tight-binding lattice. Here, the tight-binding Hamiltonian is not only the simplest model to include the essential physics of electron propagation, but also a good approximation when the lattice is fine enough compared with the electron wavelength.

The calculational procedure is as follows. An example of the system is the T -like structure as shown in the inset to Fig. 1(a). This system is divided into three parts—a box and two leads—as indicated by the dotted lines. The unperturbed Hamiltonian corresponds to the transfer terms *within* each of the three parts. The perturbation Hamiltonian corresponds to the transfer terms which *connect* these three parts. The exact (unperturbed) Green functions for each part are calculated analytically, and they are connected to construct the Green function for the total system by using the Dyson equation twice. The transmission matrix is then evaluated from the Green function,¹¹ and the Landauer formula¹² is used to obtain the conductance for the system. Note that to calculate the local density of states at any slice in the wire, the sys-

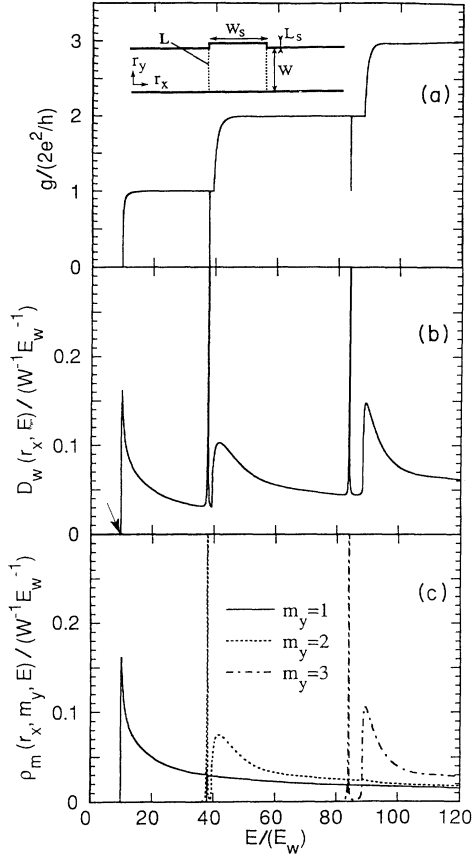


FIG. 1. (a) Conductance profile, (b) local density of states per unit length $D_w(r_x, E)$ (the arrow shows the position of the real bound state), and (c) local density of states per unit length for each mode $\rho_m(r_x, m_y, E)$ of asymmetric wire. (a) Inset: asymmetric wire structure.

tem is divided at that slice and the Dyson equation has to be used once more.

The local density of states is directly related to the imaginary part of the diagonal element of the Green function in the coordinate representation.¹³ Denoting the retarded Green function by $G^+(\vec{r}, \vec{r}', E)$, local density of states $\rho(\vec{r}, E)$ is given by

$$\begin{aligned} \rho(\vec{r}, E) &= \sum_n \delta(E - E_n) \phi_n(\vec{r}) \phi_n^*(\vec{r}) \\ &= -\frac{1}{\pi} \text{Im} \{ G^+(\vec{r}, \vec{r}, E) \}, \quad \vec{r} = (r_x, r_y), \end{aligned} \quad (2)$$

where $\phi_n(\vec{r})$ and E_n are the complete set of orthonormal eigenfunctions and eigenvalues of the Hamiltonian H , respectively. The spin degeneracy is not included in the calculation of the local density of states.

We define the local density of states per unit length of the wire $D_w(r_x, E)$ and local density of states per unit length for modes at r_x , $\rho_m(r_x, m_y, E)$ as

$$\begin{aligned} D_w(r_x, E) &= \int dr_y \rho(\vec{r}, E) = \sum_{r_y} \rho(\vec{r}, E) \\ &= \sum_{m_y} \rho_m(r_x, m_y, E), \end{aligned} \quad (3)$$

$$\rho_m(r_x, m_y, E) = \sum_n \delta(E - E_n) \varphi_n(r_x, m_y) \varphi_n^*(r_x, m_y), \quad (4)$$

$$\varphi_n(r_x, m_y) = \sum_{r_y} f_{m_y}(r_y) \phi_n(r_x, r_y), \quad (5)$$

where $f_{m_y}(r_y)$ is the eigenfunction with respect to the transverse mode. In the tight-binding model,

$$f_{m_y}(r_y) = \left[\frac{2}{N_w + 1} \right]^{1/2} \sin \left[\frac{m_y \pi r_y}{N_w + 1} \right], \quad (6)$$

where N_w is the number of sites in the transverse direction. $\rho_m(r_x, m_y, E)$ is directly obtained from the Green function, whose elements are expressed in terms of transverse modes at r_x .

It should be noted that when the translational symmetry along the propagation direction does not hold, $D_w(r_x, E)$ is position dependent and different from the total density of states of the wire. We expected it to reflect the positional variation of the density of states in the manner we observed in 1D systems. Moreover, $\rho_m(r_x, m_y, E)$ can also be used to investigate the electron properties of the quasi-one-dimensional wire.

In the present study, the units of length and energy are taken to be the width of wire W and E_w [$= \hbar^2 / (2m^* W^2)$], respectively. When the width of the wire W is 50 nm, the unit of energy is about 0.23 meV for the effective mass m^* of GaAs ($0.067m_0$), where m_0 is the electron rest mass. The unit of the local density of states per unit length is thus $(W^{-1} E_w^{-1}) = (8.7 \times 10^5 \text{ cm}^{-1} \text{ meV}^{-1})$. Note also that the energy is measured from the minimum of the two-dimensional tight-binding band, which is located under the propagation threshold in the lead. In the tight-binding lattice, we used 40 lattice spacings for the width of the semi-infinite leads. We confirmed that there is no considerable change in the result even for a finer tight-binding lattice in the low-energy range of the energy band.

We employed both asymmetric [inset to Fig. 1(a)] and symmetric [inset to Fig. 3(a)] structures to investigate the effects of geometry on the transport properties of the quantum wire. In all cases, the mismatch of width is assumed to be small so that only the transverse wavelengths of modes, which have the same mode index, have considerable matrix elements at the connection. Thus mode mixing is small and the picture that transverse modes propagate independently holds approximately.

First, we investigate the asymmetric widening of the wire [see inset to Fig. 1(a)]. The discontinuity of width is 5% the width of the wire (W). This structure may be regarded as a short stub with width W_s attached to the wire. The width of this stub W_s is equal to W . The calculated conductance, g , for this structure is plotted in Fig. 1(a). A few narrow dips are observed in the conductance profile in addition to the well-known steplike structure due to the conductance quantization. The origin of these dips can be explained by examining the local density of states. The local density of states $D_w(r_x, E)$ at L is plotted in Fig. 1(b). A few sharp peaks in addition to the quasi-one-dimensional subband spectrum are seen at the energies where the dips in Fig. 1(a) are located. The local

density of states for mode $\rho_m(r_x, m_y, E)$ is also shown for each mode m_y [see Fig. 1(c)]. There exists an almost *discrete* spectrum under the threshold energy of the continuous spectrum, which is proportional to $(\varepsilon - \varepsilon_n)^{-1/2}$ (ε_n is the threshold energy of the n th subband). This is similar to the case described by Economou,¹³ in which attractive impurity is placed in the purely one-dimensional wire. The attractive impurity makes the bound states split off from the continuous spectrum. In our work, the fact that the increase of the width lowers the energy levels for each transverse mode corresponds to the attractive potential he described.

It is very important to note that the *discrete* spectrum has a finite width [see Figs. 1(b) and 1(c)], which represents the intrinsic difference from the one-dimensional case and implies that the state in this spectrum is the quasibound state, and not the real bound state. This width becomes narrower as the stub length becomes shorter. As described above, the independent propagation of modes is an approximation and there is a finite coupling (matrix elements) between modes. Therefore, the *bound states* (if modes decouple) of the upper modes have finite probabilities of decaying to the extended states of lower modes and thus have a finite lifetime and are not perfectly localized. Considering the lower mode, the extended state becomes a complete backscattering state. This is the source of the dip structure in the conductance profile. The lifetime of the quasibound state is thus governed by the size of the mode coupling. As the mismatch of width becomes smaller, the size of the coupling to the other modes becomes smaller and the resulting lifetime becomes longer. The exception is the lowest mode. Because the bound state of the first mode does not have any lower mode to decay to, the bound state still remains as a real bound state, not the quasibound state.^{8,9} These real bound states are what Schult *et al.*¹⁴ and Sols *et al.*⁴ described. The energy of the real bound state is evaluated from the singularity of the real diagonal part of the Green function and shown by an arrow in Fig. 1(b) just below the threshold of the first propagating mode. The reason real bound states are not seen in the profile will be explained below.

Around the stub region, the quasibound state has a dominant amplitude compared with the other states. The properties of these states become clear when $\rho_m(r_x, m_y, E)$ is plotted along the propagation direction. For the peak of the discrete spectrum ($E = 38.03$) in Fig. 1(c), $\rho_m(r_x, m_y, E)$ for $m_y = 1$ and $m_y = 2$ are plotted in Fig. 2(a). Note that the r_x is measured from the center of the stub and the stub region is $-\frac{1}{2} \leq r_x \leq \frac{1}{2}$. For the second mode ($m_y = 2$), the amplitude of $\rho_m(r_x, m_y, E)$ is almost localized around the stub region. For the first mode ($m_y = 1$), the state is a standing wave with nodes. It is now clear that the second mode is the quasibound state and the first mode is the complete backscattering state. For comparison, $\rho_m(r_x, m_y, E)$ for the continuous spectrum ($E = 40.00$) is also plotted in Fig. 2(b). The states have finite amplitudes throughout the wire and have no nodes.

The effects of mode couplings discussed above become

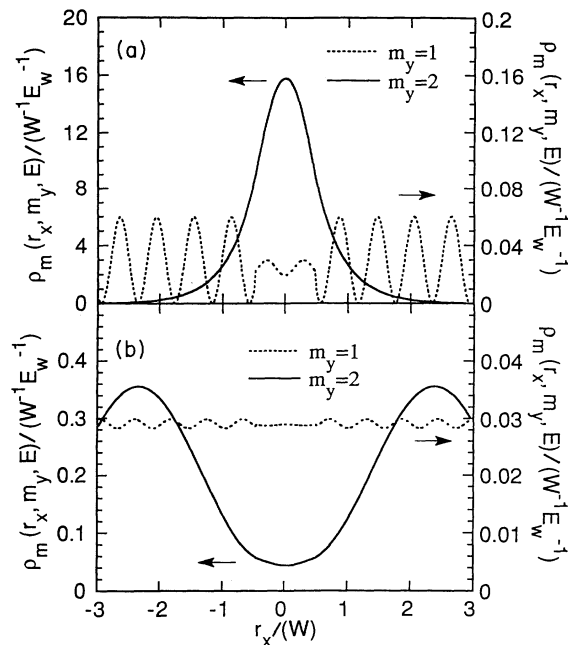


FIG. 2. Distribution of local density of states per unit length $\rho_m(r_x, m_y, E)$ about the position r_x for two energies: (a) $E = 38.03$ and (b) $E = 40.00$, both for $m_y = 1$ (dotted line) and $m_y = 2$ (solid line). Note that the scale is different for the left and right sides and that the stub region is $-\frac{1}{2} \leq r_x \leq \frac{1}{2}$.

clearer when one considers a symmetric stub structure as shown in the inset to Fig. 3(a). The mismatch of the wire width is 5% and is the same as that of the asymmetric case considered above, which means $2L'_s = L_s$. W_s is

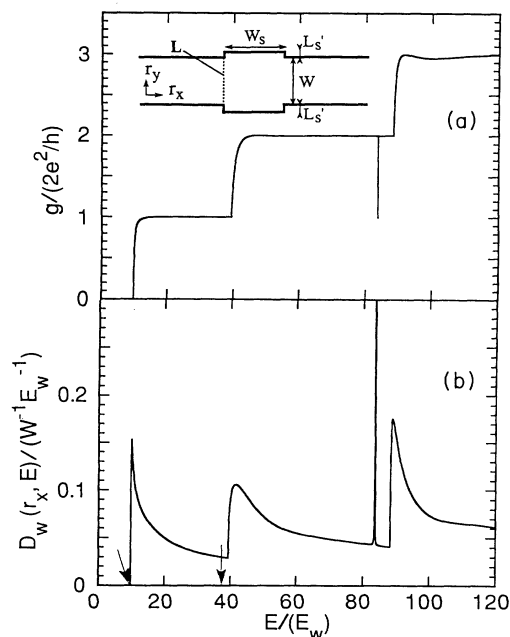


FIG. 3. (a) Conductance profile and (b) local density of states per unit length $D_w(r_x, E)$ of symmetric wire. (Arrows show the position of real bound states.) (a) Inset: symmetric wire structure.

equal to W . The conductance and the local density of states per unit length is shown in Figs. 3(a) and 3(b), respectively. The apparent difference from the asymmetric structure is the absence of the dip in the first step in Fig. 3(a). The quasibound state of the second mode is also absent in Fig. 3(b). In this structure, symmetric modes ($m_y=1,3,5,\dots$) do not couple with antisymmetric modes ($m_y=2,4,6,\dots$) in the absence of a magnetic field. Therefore, the bound state of the second mode has an infinite lifetime and still remains as a real bound state, though it has the same energy as the extended state of the first mode. The extended state is not affected and thus conductance has no dip structures in the first step. The locations of the real bound states for the first and second modes are shown by the arrows in Fig. 3(b). When the magnetic field is introduced in this structure, symmetry breaks down and a quasibound state appears again as reported by Kasai *et al.*⁵ and Schult *et al.*¹⁵

A similar situation occurs when a flat potential well is introduced inside a uniform ballistic wire. If the *form* of the confining potential is the same throughout the wire, the modes are well defined and they do not couple. As a result, a bound state of each mode cannot decay into another mode and it also remains as a real bound state. Therefore, no dips are found in the conductance profile and the conductance is given by the sum of each propagating mode. If the introduced potential makes mode couplings, however, dip structures appear. As the attractive potential becomes weaker, mode couplings become smaller and the dips become sharper as described by Chu and Sorbello.⁷

We would like to comment here on why the real bound states are not found in the calculation of the local density of states $D_w(r_x, E)$ directly. In the tight-binding Green-function calculation, the continuous function is used for both real and imaginary parts of the retarded Green function for the continuous spectrum (infinite leads). For the discrete spectrum (the box of the tight-binding lattice), however, just the real part $1/(E - E_a)$ is used for the retarded Green function, instead of $1/(E - E_a + i\delta)$.¹⁶ This difference has an effect only when the pole of the Green function is located exactly on the real axis in the complex energy plane, because otherwise the δ can be taken to be 0. This is the reason real bound states are not found in this calculation. The existence of real bound states, however, can be verified from the singularity of the real diagonal part of the Green function, as indicated by the arrows in Figs. 1(b) and 3(b).

Finally, we would like to discuss the smooth variation of wire width. In a point-contact geometry, smoothing the change of the width of the wire results in the adiabatic mode conversion that makes conductance profile a clear steplike structure.¹⁷ In case of an increase, the mode coupling becomes smaller as the variation of the width becomes slower. The width of the quasibound state then decreases and the lifetime becomes longer, and those states become close to the real bound states. This means that smooth variation of the width never removes either the quasibound states or the real bound states, though the lifetime of quasibound states becomes infinitely long in the limit of adiabatic variation. This situation is analogous to the case of a one-dimensional potential well; that is, no matter how smooth the potential well may be, the bound states cannot be removed as long as the potential has a finite depth. Moreover, it is well known that a bound state exists for infinitesimal attractive potential in one dimension.¹³ Thus bound and quasibound states exist for an infinitesimally increased wire.

Our evaluation of the local density of states per unit length and the conductance permits a comparison of the static and dynamic electronic properties in a quasi-one-dimensional system, and it will also be very useful when other geometries, such as the point-contact or the double-constriction structure, are considered. We also investigated the longer-stub structure and found that the quasibound states are also well defined when the propagating modes are not defined even approximately through the wire.¹⁸

In conclusion, we have investigated the electronic properties of ballistic quantum wires with a small width increase. The local density of states per unit length and the conductance were calculated by the tight-binding Green-function method. Our examination of the local density of states in the quantum wires clearly reveals that the quasibound state and the complete backscattering state arise as a result of mode coupling and that this is the origin of the dip structures in the conductance. We also conclude that smooth variation of the wire width cannot remove quasibound or real bound states.

The authors would like to thank M. Yamamoto, Y. Tokura, and F. Sols for helpful discussions and K. Hirata for his encouragement. One of the authors (T.I.) would like to thank S. Sugitani and K. Asai for providing him with much valuable advice.

¹B. J. van Wees, H. van Houten, C. W. J. Beenakker, J. G. Williamson, L. P. Kouwenhoven, D. van der Marel, and C. T. Foxon, *Phys. Rev. Lett.* **60**, 848 (1988); D. A. Wharam, T. J. Thornton, R. Newbury, M. Pepper, H. Ahmed, J. E. F. Frost, D. G. Hasko, D. C. Peacock, D. A. Ritchie, and G. A. C. Jones, *J. Phys. C* **21**, L209 (1988).

²A. Szafer and A. D. Stone, *Phys. Rev. Lett.* **62**, 300 (1989).

³A. Weisshaar, J. Lary, S. M. Goodnick, and V. K. Tripathi, *Appl. Phys. Lett.* **55**, 2114 (1989).

⁴F. Sols, M. Macucci, U. Ravaioli, and K. Hess, *J. Appl. Phys.* **66**, 3892 (1989).

⁵H. Kasai, K. Mitsutake, and A. Okiji, *J. Phys. Soc. Jpn.* **60**, 1679 (1991).

⁶K. Nakazato and R. J. Blaikie, *J. Phys. Condens. Matter* **3**, 5729 (1991).

⁷C. S. Chu and R. S. Sorbello, *Phys. Rev. B* **40**, 5941 (1989).

⁸P. F. Bagwell, *Phys. Rev. B* **41**, 10354 (1990).

⁹E. Tekman and S. Ciraci, *Phys. Rev. B* **43**, 7145 (1991).

- ¹⁰D. J. Thouless and S. Kirkpatrick, *J. Phys. C* **14**, 235 (1981); P. A. Lee and D. S. Fisher, *Phys. Rev. Lett.* **47**, 882 (1981).
- ¹¹D. S. Fisher and P. A. Lee, *Phys. Rev. B* **23**, 6851 (1981); A. D. Stone and A. Szafer, *IBM J. Res. Develop.* **32**, 384 (1988).
- ¹²R. Landauer, *IBM J. Res. Develop.* **32**, 306 (1988).
- ¹³E. N. Economou, *Green's Functions in Quantum Physics* (Springer-Verlag, Berlin, 1983).
- ¹⁴R. L. Schult, D. G. Ravenhall, and H. W. Wyld, *Phys. Rev. B* **39**, 5476 (1989).
- ¹⁵R. L. Schult, H. W. Wyld, and D. G. Ravenhall, *Phys. Rev. B* **41**, 12 760 (1990).
- ¹⁶H. U. Baranger, D. P. DiVincenzo, R. A. Jalabert, and A. D. Stone, *Phys. Rev. B* **44**, 10 637 (1991).
- ¹⁷L. I. Glazman, G. B. Lesovik, D. E. Khmel'nitskii, and R. I. Shekhter, *Pis'ma Zh. Eksp. Teor. Fiz.* **48**, 218 (1988) [*JETP Lett.* **48**, 238 (1988)].
- ¹⁸T. Itoh, N. Sano, and A. Yoshii (unpublished).